Simulation of Light Absorption in Tumor-Embedded Prostate for Transurethral Light Delivery by Diffusing Light

Peng Dongqing[1,2] Li Hui[1]

[1]*Key Laboratory of Optoelectronic Science and Technology for Medicine of Ministry of Education, Fujian Provincial Key Laboratory of Photonic Technology, College of Photonic and Electronic Engineering, Fujian Normal University, Fuzhou, Fujian* 350007, *China*

[2]*School of Science, Jimei University, Xiamen, Fujian* 361021, *China*

Abstract Photoacoustic imaging has recently emerged as a promising imaging modality for prostate cancer. Knowledge of absorbed light distribution in prostate tissues is essential since the distribution characteristics of absorbed light energy will influence the imaging depth and range of photoacoustic imaging (PAI). In this paper, a tumor-embedded prostate optical model was established. Light absorption distribution patterns of the tissue model through trans-urethral laser illumination using cylindrical diffusing light (CDL) and spherical diffusing light (SDL) were studied based on the Molecular Optical Simulation Environment (MOSE). In addition, the influence of laser energy and absorption coefficient of tumor on the light absorption in tumor was demonstrated. The results show that laser illumination from urethral allows the prostate tissues to obtain more efficient light absorption. The light absorption distribution of tumors irradiated by CDL has a relatively uniform characteristic in a large range, with its value around the light source less than that of SDL. Laser energy and tumor absorption coefficient has linear effect on the light absorption of tumor, which is consistent with the Beer Law. The conclusions will be helpful to optimize the laser source and to improve the imaging depth in a photoacoustic imaging system.

Key words medical optics; Molecular Optical Simulation Environment; light absorption; diffusing source; prostate cancer; photoacoustic imaging

OCIS codes 170.3660; 170.5120; 170.5280

弥散光经尿道辐照时嵌肿瘤前列腺组织内部光吸收的模拟研究

彭东青[1,2] 李 晖[1]

[1]福建师范大学光电与信息工程学院医学光电科学教育部重点实验室, 光子技术福建省重点实验室, 福建 福州 350007

[2]集美大学理学院, 福建 厦门 361021

摘要 光声成像技术近年来已成为一种极具前景的前列腺癌成像技术。由于光声成像范围与光能量的吸收分布直接相关,为了优化经尿道光辐照的前列腺光声成像系统的光源参数,必须了解前列腺组织的光吸收分布。根据前列腺组织的形态特征构建了一个嵌有球状肿瘤的三维前列腺光学模型,利用光学分子影像仿真平台(MOSE)比较研究了柱状和球状两种弥散光源经尿道辐照时组织内光吸收分布特性。考查了激光能量和肿瘤处光学吸收系数对肿瘤光吸收的影响。模拟结果表明经尿道照明有利于前列腺组织内部光吸收,特别是深处位置。另外,相比于球状弥散光源,柱状弥散光源侧向光吸收分布较均匀,适合于三维扫描光声成像和信源分析。研究结果表明增大输入的激光能量或者肿瘤光学吸收系数可以明显提高肿瘤处光能量吸收,这与组织光学中的有关理论一致。有关结论有助于前列腺光声成像系统的光源优化设计和成像深度的改善。

收稿日期: 2015-06-12; **收到修改稿日期**: 2015-08-13; **网络出版日期**: 2015-10-27

基金项目: 国家自然科学基金(61178089,81201124)、福建省科技计划重点项目(2011Y0019)、福建省教育厅科技计划(JA14189)、医学光电科学教育部重点实验室开放课题(JYG1417)

作者简介: 彭东青(1978—),男,博士研究生,讲师,主要从事组织光学和光声成像技术等方面的研究。

E-mail: dqpeng@jmu.edu.cn

导师简介: 李 晖(1963—),男,博士,教授,主要从事生物医学光子技术方面的研究。

E-mail: hli@fjnu.edu.cn (通信联系人)

关键词 医用光学; 光学分子影像仿真; 光吸收; 弥散光源; 前列腺肿瘤; 光声成像
中图分类号 O436 文献标识码 A
doi: 10.3788/LOP52.121703

1 Introduction

In recent years, prostate cancer has been a serious health concern around the world, especially in the United States[1-2]. Photoacoustic imaging (PAI) has recently emerged as a promising imaging modality for various biomedical applications[3], which combines the contrast capability of optical imaging with the resolution of ultrasound imaging. Some studies have demonstrated that PAI can be used as a tool for imaging prostate lesion[4-7]. Trans-rectal light illumination combined with ultrasound transducer has been a usual imaging model in the previous PAI studies[5], but it was difficult to improve accuracy in the reconstructed image because trans-rectal light illumination was suffering from the great light absorption attenuation of the rectal wall. Xie *et al.*[8] presented a photoacoustic imaging technique for prostate cancer based on trans-urethral laser illumination using diffuse light source. As we know, the temporal amplitude and profile of photoacoustic signals are spatial mappings of the absorbed optical energy. The distribution characteristic of absorbed light energy would determine the imaging depth and range of PAI. In order to optimize light delivery in photoacoustic imaging, Monte Carlo simulation for light transport in tissues has been carried out[9-11]. However, so far a complex optical model of tumor-embedded prostate tissue internally irradiated by diffusing light source was not available. In order to gain deeper understanding of light absorption characteristics and optimize the light absorption inside the tumor-embedded prostate tissue through trans-urethral laser illumination using diffuse light source, a 3D tumor-embedded prostate optical model was established according to the structure of human prostate. And the propagation characteristics and light distribution patterns in the tissue model irradiated by two different diffusing light sources through urethral were studied and compared between each other based on the latest published Monte Carlo software named Molecular Optical Simulation Environment (MOSE 2.3)[12-15]. In addition, the effect of the laser energy and absorption coefficient of tumor on the light absorption energy in tumor was demonstrated. The conclusions help to optimize the laser source in a photoacoustic imaging system.

2 Model and method

It was known to all the prostate looks like a chestnut with transversal diameter, longitudinal diameter and the vertical diameter of about 4, 2 and 3 cm, respectively. Clinical examination showed that prostate tumor often happened in the lobe of posterior. Solid tumors have increased blood flow, and therefore hemoglobin concentration rises. As a result, there was high optical absorption of tumor compared with other normal tissue components at wavelengths in the visible and near-infrared range.

Taking into account the location of ultrasound probe for photoacoustic signal detection in rectum, trans-urethral laser illumination was adopted using diffuse light source, a 3D triangular meshes tumor-embedded prostate optical model was established based on human prostate morphology through programming, as shown in Fig. 1. Three spherical absorbers with the same high optical absorption coefficient at three different positions were set to simulate tumors. The triangular meshes were expressed as OFF files. The OFF file used the surface of object to represent the geometry of the object, then the surface of the object was divided into a large number of triangles. The prostate phantom′s transversal diameters in x-axis, y-axis and the height were 2, 3. 8, 3. 184 cm, respectively, and its center was located at (0,0,15.92) mm. Diameters of the three tumors were all set to 2 mm, and the location was (2,0,16) mm for tumor-1, (5,0,16) mm for tumor-2, and (2,0,9) mm for tumor-3. The Cartesian coordinates were used for the simulation.

According to optical properties of human prostate from foreign group[16-17], main optical parameters

including absorption coefficient μ_a, scattering coefficient $\mu_s'=\mu_s(1-g)$ where g is anisotropy, and tissue refractive index n at 732 nm for prostate optical model and the three tumors are listed in table 1.

Table 1 Optical parameters of simulation model

Tissue	μ_a /mm^{-1}	μ_s /mm^{-1}	g	n
Prostate	0.03	3.8	0.95	1.43
Tumor-1	0.3	4.5	0.97	1.40
Tumor-2	0.3	4.5	0.97	1.40
Tumor-3	0.3	4.5	0.97	1.40

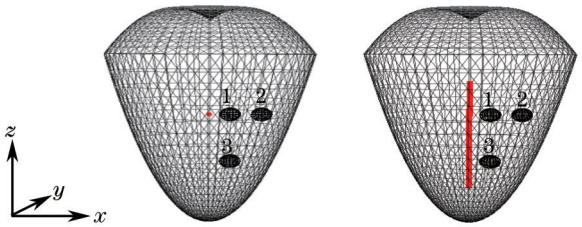

Fig.1 A 3D tumor-embedded prostate model using trans-urethral laser illumination. (a) By spherical diffusing light (SDL); (b) by cylindrical diffusing light (CDL)

Two kinds of diffusing laser light sources were employed to simulate the trans-urethral laser illumination, one was SDL with the diameter of 0.6 mm and its center was located at x=0, y=0, z=16 mm, as illustrated in Fig. 1(a); the other was CDL with the diameter of 0.6 mm, the effective light length was 16 mm, and its center was at x=0, y=0, z=13 mm, as illustrated in Fig. 1(b). The wavelength of these two light sources was set to 732 nm since the depth of penetration at 732 nm was much larger than that at other wavelengths. The total energy of incident light was all set to 1 J.

Because the Boltzmann equation was too difficult to be solved directly using analytic method, the Monte Carlo (MC) simulation, as a numerical method, was now commonly used to calculate the light distribution in tissues, especially suitable for the study of tissues with complex structure[18-22]. Studies have shown that the MC result can be legitimately considered as the low-noise version of the actual physical measurement. Recently, some simulation softwares of codes have been developed based on the MC method, in which MOSE has several significant features, such as supporting the description of the medium with a regular shape (ellipse, rectangle) under 2D, regular shape (ellipsoid, cylinder, cube) under 3D and irregular shape (the boundary is described by a triangle mesh; for example, data in PLY, OFF, SURF, MESH, and AM formats), and it is helpful for users to implement the MC simulation under a complex medium. It is more notable that the accuracy of the simulation from MOSE was validated by real experiments[14-15].

In this section, the abstract optical model was combined with MOSE 2.3 to investigate light absorption distribution in prostate tissues irradiated by these two diffusing light sources. The record range of light distribution in the process of simulation was (-10 mm, 10 mm) in x-axis, (-19 mm, 19 mm) in y-axis, (0, 31.84 mm) in z- axis; and the record step was set to 0.2, 0.38 and 0.3184 mm, respectively. The total incident photon number was 500000.

3 Results and discussion

The light absorption results for the tumor-embedded prostate model were shown in Fig. 2 and Fig. 3, in which Figs. 2(a) and 3(a) were for yz-plane; and Figs. 2(b) and 3(b) were for xz-plane. The light absorption in all figures represents the logarithm of absorbed energy. It can be seen that light absorption happened everywhere in the prostate tissue model by using trans-urethral laser illumination. It is worth noting that there was symmetrical light absorption around the light source. It indicates that laser illumination from urethral can allow the prostate tissues to obtain more efficient light absorption, particularly at deep positions.

Comparing Fig. 2(a) with Fig. 2(b), it is found that the lateral distribution scope of uniform light absorption within the prostate model through CDL illumination is much larger than that through SDL illumination. The absorbed light energy near light source is lower, which can avoid heat damage of normal tissues. The difference between Fig. 3(a) and Fig. 3(b) is similar to that between Fig. 2(a) and Fig. 2(b). But the light distribution range at xz−plane is much smaller than that at yz−plane. It can be explained as the influence of boundary reflected by the photons. As the prostate tumor occurred mainly in the posterior lobe near the xz−plane, the absorbed light energy at xz−plane was selected for further analysis.

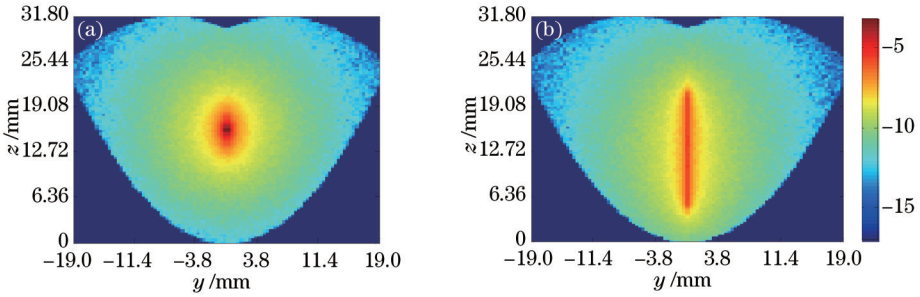

Fig.2 Light absorption distribution of the tumor−embedded prostate model produced by two light sources at yz−plane (x=0). (a) SDL; (b) CDL

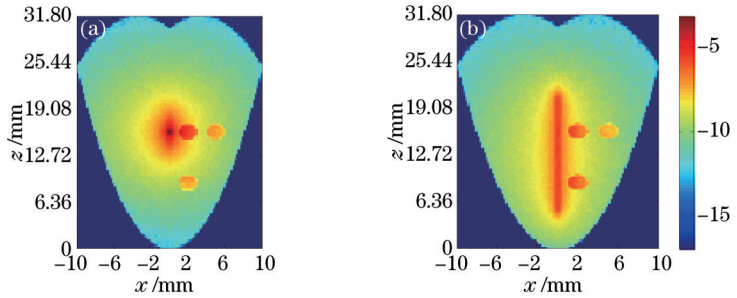

Fig.3 Light absorption distribution of the tumor−embedded prostate model produced by two light sources at xz−plane (y=0). (a) SDL; (b) CDL

In Fig. 3, strong light energy absorption at three spherical absorbers was observed compared to surrounding normal prostate tissues. With regard to CDL, absorbed light energy in tumor−1 is the same as that in tumor−2. However, absorbed light energy in tumor−1 is much larger than that in tumor−2, in which SDL was used. The difference also exists between Fig. 4(a) and Fig. 4(b), which represent the light absorption distribution of the tumor−embedded prostate model at the yz−plane where x=2 mm. In addition, light absorption of tumor−3 decreases both in Fig. 3(a) and Fig. 3(b).

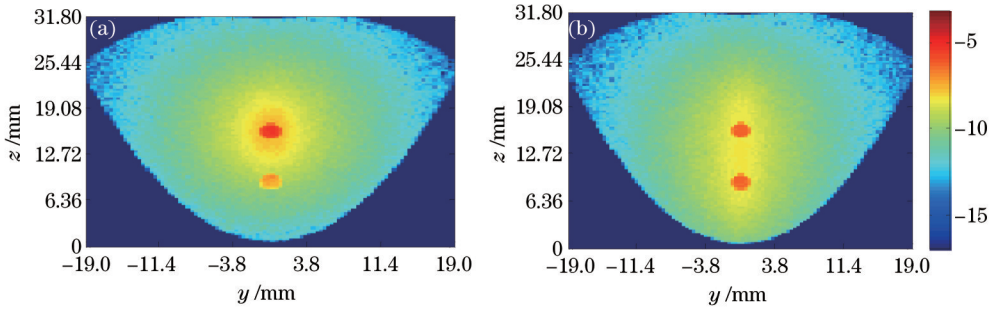

Fig. 4 Light absorption distribution of the tumor−embedded prostate model produced by two light sources at yz−plane (x=2 mm). (a) SDL; (b) CDL

In order to give further comparison of light absorption distribution of the two diffusing light sources, absorbed light energy distribution profiles through tumor center along z direction and x direction are shown in Fig. 5(a) and Fig. 5(b), respectively.

The absorbed intensity profiles along z direction or x direction both reveal the tumor boundary, and the tumor size can be determined by the curves. Fig. 5(a) illustrates that the light absorption in tumor-1 is almost the same as that in tumor-2 since there is a larger distribution range of uniform light absorption irradiated by CDL. But light energy absorption in the two tumors is quite different when they were irradiated by SDL. Absorbed light energy in tumor-1 is much higher than that in tumor-2. Furthermore, whether irradiated by SDL or CDL, light absorption in tumor-1 decreases to that in tumor-2 according to the exponential decay. As we know, the function of the light fluence $F(x)$ on the tissue and the depth x agrees with the Beer Law, which states $F(x)=F_0\exp(-\mu_t x)$, where F_0 is the initial light fluence, μ_t is the total attenuation coefficient of the tissue. When x increases, the light fluence $F(x)$ will decrease according to above equation, thus the light absorption energy $A(x)=\mu_a F(x)$ in tumor decreases since the optical coefficient of tumor is equivalent.

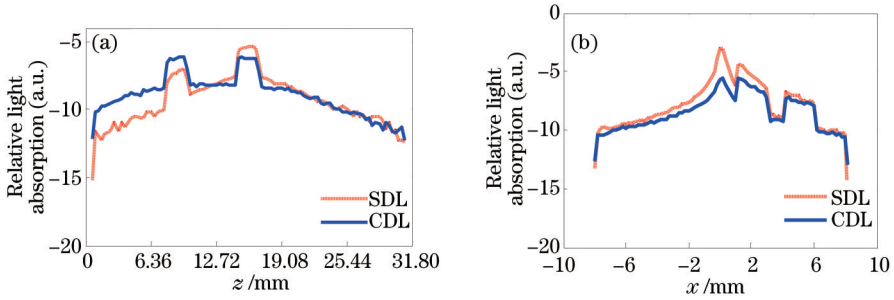

Fig.5 Profiles of absorbed light energy distribution. (a) Along z direction through center of tumor-1 (x=2 mm); (b) along x direction through center of tumor-1 (z=16 mm)

The results hint that light energy absorption of tumors irradiated by SDL is significantly different at different locations, which is not conducive to 3D scanning of PAI, as well as the analysis of variance between photoacoustic signal and light source. But light energy absorption of tumors irradiated by CDL is roughly uniform in a large range. Since absorbed light energy by CDL along x direction is less than that by SDL, increase of laser energy of CDL is allowed for further imaging depth whereas the normal tissue is not destroyed. Therefore, the CDL was used for the following simulation.

Relationship between absorbed light energy in two tumors and laser energy is shown in Fig. 6(a) for tumor-1 centered at (2,0,16) mm and Fig. 6(b) for tumor-2 centered at (5,0,16) mm. Relatively linear relationship

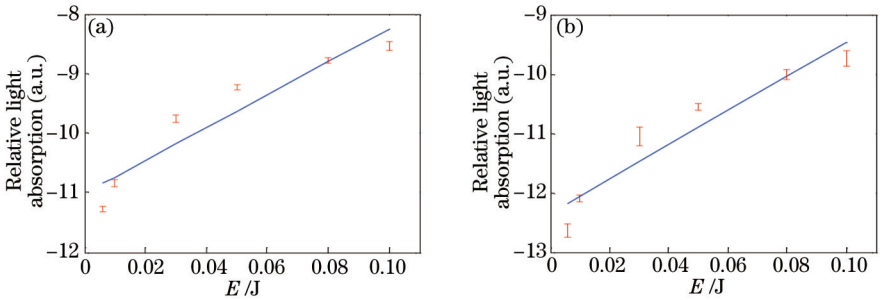

Fig.6 Relationship between light absorption in tumor and laser energy. (a) Tumor-1; (b) tumor-2

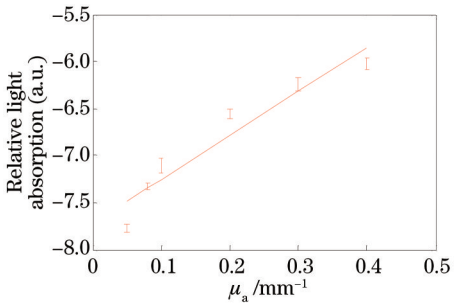

Fig.7 Relationship between light absorption in tumor and absorption coefficient of tumor

between light absorption and incident laser energy is observed. Likewise, Fig. 7 indicates that there also exists relatively linear relationship between light absorption energy and absorption coefficient of tumor. Fig. 6 and Fig. 7 can also be easily interpreted by the Beer′s Law, and show the reliability of the simulation. Thus the imaging depth of PAI may be improved by increasing laser energy or using contrast agents which can enhance the optical absorption properties of tumor tissues.

4 Conclusion

The numerical simulation of a 3D optical model of a complex structure bio-tissue will be useful for quantitative prediction of the light absorption distribution for optical imaging in biomedicine. A tumor-embedded prostate optical model was employed combined with a latest published simulation platform MOSE to provide the light absorption distribution in the prostate tissue through trans-urethral laser illumination using CDL and SDL. In addition, the effect of the laser energy and absorption coefficient of tumor on the light absorption energy in tumor was demonstrated. The results show that laser illumination from urethral will allow the prostate tissue to obtain more efficient light absorption than trans-rectal light illumination, particularly at deep position. Light absorption distribution of tumors irradiated by CDL has a relatively uniform characteristic in a large range, with its value around the light source less than that of SDL. It indicates that the CDL source is more suitable for the 3D scanning of PAI than SDL. Laser energy and tumor absorption coefficient has linear effect on the light absorption of tumor, which is consistent with the diffusion theory. Therefore laser energy of cylindrical diffusing light source should be raised appropriately without worrying about heat damage of normal tissue around light source, and contrast agents which can enhance the optical absorption properties of tumor tissues may be used in order to further imaging depth. These conclusions will be helpful to optimize the laser delivery modality in a photoacoustic imaging system.

Reference

1 Dogra V S, Chinni B K, Valluru K S, *et al*.. Multispectral photoacoustic imaging of prostate cancer: Preliminary *ex-vivo* results[J]. J Clin Imaging Sci, 2013, 3(3): 41-48.

2 Siegel R, Ma J M, Zou Z H, *et al*.. Cancer statistics, 2014 [J]. Ca-Cancer J Clin, 2014, 64(1): 9-29.

3 Li C, Wang L. Photoacoustic tomography and sensing in biomedicine[J]. Phys Med Biol, 2009, 54(19): R59-R97.

4 Wang X, Roberts W W, Carson P L, *et al*.. Photoacoustic tomography: A potential new tool for prostate cancer[J]. Biomed Opt Express, 2010, 1(4): 1117-1126.

5 Yaseen M A, Ermilov S A, Brecht H P, *et al*.. Optoacoustic imaging of the prostate: Development toward image-guided biopsy[J]. J Biomed Opt, 2010, 15(2): 021310.

6 Su J L, Bouchard R R, Karpiouk A B, *et al*.. Photoacoustic imaging of prostate brachytherapy seeds[J]. Biomed Opt Express, 2011, 2(8): 2243-2254.

7 Bell M A L, Kuo N, Song D Y, *et al*.. Short-lag spatial coherence beamforming of photoacoustic images for enhanced visualization of prostate brachytherapy seeds[J]. Biomed Opt Express, 2013, 4(10): 1964-1977.

8 Xie W, Li Z, Li H. Photoacoustic imaging of prostate cancer using cylinder diffuse radiation[C]. SPIE, 2012, 8553: 85532V.

9 Periyasamy V, Pramanik M. Monte Carlo simulation of light transport in tissue for optimizing light delivery in photoacoustic imaging of the sentinel lymph node[J]. J Biomed Opt, 2013, 18(10): 106008.

10 Stantz K M, Liu B, Kruger R A. Using Monte Carlo simulations to understand the influence of photon propagation on photoacoustic spectroscopic imaging[C]. SPIE, 2007, 6437: 64370Z.

11 El-Gohary S H, Metwally M K, Eom S, *et al*.. Design study on photoacoustic probe to detect prostate cancer using 3D Monte Carlo simulation and finite element method[J]. Biomed Eng Lett, 2014, 4(3): 250-257.

12 Ren S, Chen X, Wang H, *et al*.. Molecular optical simulation environment (MOSE): A platform for the simulation of light propagation in turbid media[J]. PLoS ONE, 2013, 8(4): e61304.

13 Ren N, Liang J, Qu X, *et al*.. GPU-based Monte Carlo simulation for light propagation in complex heterogeneous tissues [J]. Opt Express, 2010, 18(7): 6811-6823.

14 Li H, Tian J, Zhu F P, *et al*.. A mouse optical simulation environment (MOSE) to investigate bioluminescent phenomena in the living mouse with the Monte Carlo method[J]. Acad Radiol, 2004, 11(9): 1029-1038.

15 Chen X, Gao X, Qu X, *et al*.. A study of photon propagation in free-space based on hybrid radiosity-radiance theorem [J]. Opt Express, 2009, 17(18): 16266-16280.

16 Zhu T C, Dimofte A, Finlay J C, *et al*.. Optical properties of human prostate at 732 nm measured *in vivo* during motexafin lutetium-mediated photodynamic therapy[J]. Photochem Photobiol, 2005, 81(1): 96-105.

17 Zhu T C, Hahn S M, Kapatkin A S, *et al*.. *In vivo* optical properties of normal canine prostate at 732 nm using motexafin lutetium-mediated photodynamic therapy[J]. Photochem Photobiol, 2003, 77(1): 81-88.

18 Chen Yanping, Li Chunbin, Wang Xiaoling, *et al*.. Detection of knee osteoarthritis with near infrared spectroscopy *in vivo*[J]. Journal of Optoelectronics·Laser, 2014, 25(5): 1023-1026.
陈延平, 李纯彬, 王晓玲, 等. 膝骨性关节炎在体近红外光谱检测[J]. 光电子·激光, 2014, 25(5): 1023-1026.

19 Yang Bozan, Yang Chunmei, Sa Yu, *et al*.. Simulation and experimental studies of heterogeneous turbid medium by multispectral reflectance imaging[J]. Journal of Optoelectronics·Laser, 2014, 25(12): 2437-2446.
杨博赞, 杨春梅, 撒 昱, 等. 非均匀混浊介质多光谱反射成像的仿真与实验研究[J]. 光电子·激光, 2014, 25(12): 2437-2446.

20 Peng D, Xie W, Guo J, *et al*.. Light absorption distribution of prostate tissue irradiated by diffusing light source[J]. Optoelectron Lett, 2015, 11(3): 237-240.

21 Zhang Yong, Chen Bin, Li Dong. A three-dimensional geometric Monte Carlo method for simulation of light propagation in biological tissues[J]. Chinese J Lasers, 2015, 42(1): 0104003.
张 永, 陈 斌, 李 东. 一种模拟生物组织内光传播的三维几何蒙特卡罗方法[J]. 中国激光, 2015, 42(1): 0104003.

22 Jia Hao, Chen Bin, Li Dong, *et al*.. Unstructured grid based Monte Carlo method for the simulation of light propagation in skin tissues[J]. Chinese J Lasers, 2015, 42(4): 0404001.
贾 浩, 陈 斌, 李 东, 等. 模拟皮肤组织中光传播的非结构化网格蒙特卡罗法[J]. 中国激光, 2015, 42(4): 0404001.

栏目编辑: 吴秀娟